



OPEN ACCESS

EDITED BY

Lin Chen,
University of Shanghai for Science and
Technology, China

REVIEWED BY

Dexian Yan,
China Jiliang University, China
Huawei Liang,
Shenzhen University, China
Fei Fan,
Nankai University, China
Kuang Zhang,
Harbin Institute of Technology, China
Guoxing Zheng,
Wuhan University, China

*CORRESPONDENCE

Ling Wang,
wangling@hnfnu.edu.cn
Li Deng,
dengl@bupt.edu.cn

SPECIALTY SECTION

This article was submitted to
Interdisciplinary Physics,
a section of the journal
Frontiers in Physics

RECEIVED 12 July 2022

ACCEPTED 16 August 2022

PUBLISHED 06 September 2022

CITATION

Wang L, Yang Y, Gao F, Teng S, Tan Z-G,
Zhang X, Lou J and Deng L (2022),
Terahertz reconfigurable dielectric
metasurface hybridized with vanadium
dioxide for two-dimensional
multichannel multiplexing.
Front. Phys. 10:992037.
doi: 10.3389/fphy.2022.992037

COPYRIGHT

© 2022 Wang, Yang, Gao, Teng, Tan,
Zhang, Lou and Deng. This is an open-
access article distributed under the
terms of the [Creative Commons
Attribution License \(CC BY\)](#). The use,
distribution or reproduction in other
forums is permitted, provided the
original author(s) and the copyright
owner(s) are credited and that the
original publication in this journal is
cited, in accordance with accepted
academic practice. No use, distribution
or reproduction is permitted which does
not comply with these terms.

Terahertz reconfigurable dielectric metasurface hybridized with vanadium dioxide for two-dimensional multichannel multiplexing

Ling Wang^{1*}, Yang Yang², Feng Gao¹, Shuhua Teng¹,
Zhi-Guo Tan¹, Xing Zhang¹, Jun Lou¹ and Li Deng^{3*}

¹School of Electronic Information, Hunan First Normal University, Changsha, China, ²School of Electrical and Data Engineering, Tech Lab, University of Technology Sydney, Sydney, NSW, Australia, ³School of Information and Communication Engineering, Beijing University of Posts and Telecommunications, Beijing, China

The metasurface hybridized with vanadium dioxide (VO₂) can be dynamically tuned, which has attracted enormous attention in recent years and orbital angular momentum (OAM) multiplexing based on metasurfaces has shown promising prospects in terahertz communications. However, existing research on VO₂ metasurface focuses on the metallic metasurface. The dielectric VO₂ metasurface used for OAM multiplexing is rarely reported to the present. This paper proposed a terahertz reconfigurable dielectric metasurface hybridized with VO₂ for two-dimensional multichannel multiplexing combining with spatial and frequency domains. The metasurface works in both reflection and transmission modes and simultaneously the polarization control and operating frequency band regulation can be realized by switching the VO₂ from the metallic state to the insulator state. For the reflective or transmissive metasurface, when 4×M-channel (M is a positive integer) off-axis plane waves are incident on the metasurface, the co-polarization reflected or cross-polarization transmitted waves are transformed into 4×M-channel orthogonal on-axis beams with topological or frequency orthogonality. A metasurface composed of 14 × 14 unit cells is designed for verification. The simulated result shows that two-dimensional 12-channel multiplexing combining with OAM and frequency by the designed metasurface can be realized on the reflection and transmission modes in two different frequency bands. The proposed metasurface has great potential in terahertz communications.

KEYWORDS

terahertz, dielectric metasurface, vanadium dioxide, multiplexing, orbital angular momentum

Introduction

The metasurface [1], as the two-dimensional metamaterial, can effectively manipulate the phase, amplitude, and polarization of electromagnetic (EM) waves and considerable effort has been devoted to investigating the metasurface. The metasurface hybridized with dynamically tunable materials, such as graphene [2], liquid crystals [3], and PIN diode [4], is called reconfigurable metasurface [5]. Compared with the fixed metasurface without active materials, EM properties of the reconfigurable metasurface can be dynamically tuned by controlling the active devices, which has attracted enormous attention in recent years. The phase-change material vanadium dioxide (VO₂) offers excellent switching behavior from insulator state to metallic state around 68°C driven by temperature, electric fields, and laser pumping in the terahertz region [6, 7]. Therefore, it is an efficient method to incorporate VO₂ into the metasurface to realize the terahertz reconfigurable metasurface. Besides, according to the primary category of materials constituting metasurface, metasurfaces can be divided into metallic and dielectric metasurfaces. The dielectric metasurface has advantages of low Ohmic loss, low cost, ultrahigh transmission efficiency, etc., compared with metallic metasurface [8]. But the existing research on VO₂ reconfigurable metasurface has been focused on the metallic metasurface. Therefore, the reconfigurable dielectric metasurface hybridized with VO₂ is worthy of being further studied.

In general, five physical domains, including time, polarization, frequency, quadrature, and space, can be used for beam multiplexing to improve the data rate and capacity of communication systems [9]. The vortex beam carrying orbital angular momentum (OAM) is characterized by the doughnut-shaped intensity profile and helical phase front. Besides, OAM beams with various topological charges are orthogonal with each other and are available for spatial multiplexing [10]. Therefore, generating the OAM beam [11–15], achieving OAM multiplexing [13, 16–23], and further realizing two-dimensional or multi-dimensional multiplexing combined with OAM and other four physical domains by metasurface [24–28], have shown promising prospects in high-speed and huge-capacity communication systems, especially in terahertz communications. However, existing VO₂ reconfigurable metasurfaces are mainly concentrated on achieving active manipulation of the transmission coefficient [29], reflection coefficient [30], planar-chiral response [31], and Mie resonant [32], or realizing dynamic polarization converter [33, 34], metalens [35], absorber [36, 37], beam splitter [38, 39], OAM generator [40], and meta-holography [41]. The VO₂ metasurface used for OAM multiplexing [42] is rarely reported to the present.

A terahertz reconfigurable dielectric metasurface embedded with VO₂ for two-dimensional multichannel multiplexing combing with spatial and frequency domains is presented in this paper. The

metasurface can simultaneously realize reflection-transmission mode switching and polarization regulation and the working frequency is controlled by easily tuning the state of VO₂ without physically changing the structure. The unit cell of the metasurface comprises a top silicon elliptical pillar and a silicon-VO₂ substrate. When the circularly polarized wave is perpendicular to the unit cell with VO₂ in the metallic and insulator states respectively, the simulation result shows that both the 3 dB bandwidth of the co-polarization reflection coefficient and the cross-polarization transmission coefficient is about 0.1 THz. Operating frequency bands are about 0.18–0.28 THz and 0.25–0.35 THz respectively. The metasurface is designed based on the method of two-dimensional multichannel multiplexing combing with spatial and frequency domains [27] and the Pancharatnam Berry (PB) phase (geometric phase) principle [43, 44]. The simulated results show that the designed metasurface can work in both reflection and transmission modes with the working frequency range of 0.18–0.28 THz and 0.25–0.35 THz respectively. By switching the state of VO₂, 12-channel orthogonal on-axis co-polarization reflected beams and cross-polarization transmitted beams with topological or frequency orthogonality are generated, when 12-channel off-axis plane waves are incident onto the dielectric metasurface. That is, two-dimensional multichannel multiplexing combing spatial and frequency domains can be achieved in both reflection and transmission mode by the proposed metasurface. The proposed metasurface has great potential in terahertz communications.

Operating principle

Figure 1 shows the schematic diagram for two-dimensional multichannel multiplexing combing spatial and frequency domains by the terahertz reconfigurable dielectric metasurface which can work in both reflection and transmission modes by tuning the VO₂.

As shown in Figure 1A, the designed metasurface works in the reflection mode. For the group 1 (channels C₁₁ to C_{1M}), *M*-channel right-handed circularly polarized (RCP) plane wave with frequency *f_m* and angle of incidence $\theta_i(f_m)$ ($m = 1, \dots, M$) obliquely illuminate the reflective metasurface from the negative *z*-axis along the $-x$ direction, in the direction perpendicular to the metasurface, the co-polarization reflected waves (RCP reflected wave) are transformed into on-axis OAM beams with *l*₁. Because frequencies of channels C₁₁ to C_{1M} are different, the generated *M*-channel on-axis OAM beams are orthogonal with each other. In the same way, for the group 2 (channels C₂₁ to C_{2M}), the group 3 (channels C₃₁ to C_{3M}), and the group 4 (channels C₄₁ to C_{4M}), the RCP plane wave with frequency *f_m* and the angle of incidence $\theta_i(f_m)$ obliquely illuminate on the reflective metasurface from the negative *z*-axis along negative *y*, positive *x*, and positive *y* directions respectively, in the direction perpendicular to the metasurface, RCP reflected waves are transformed into *M*-channel orthogonal on-axis OAM beams with *l*₂, *l*₃, and *l*₄

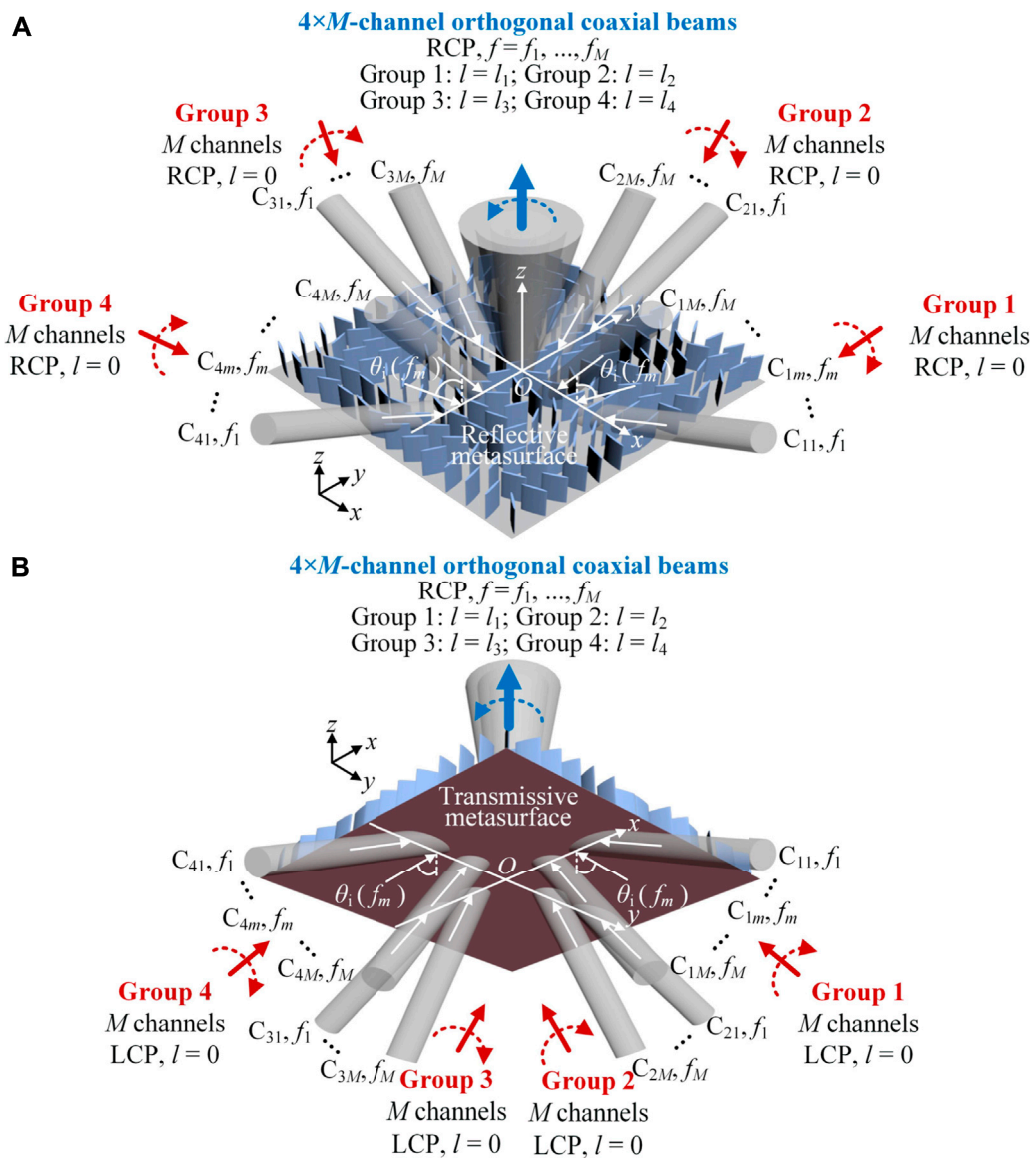
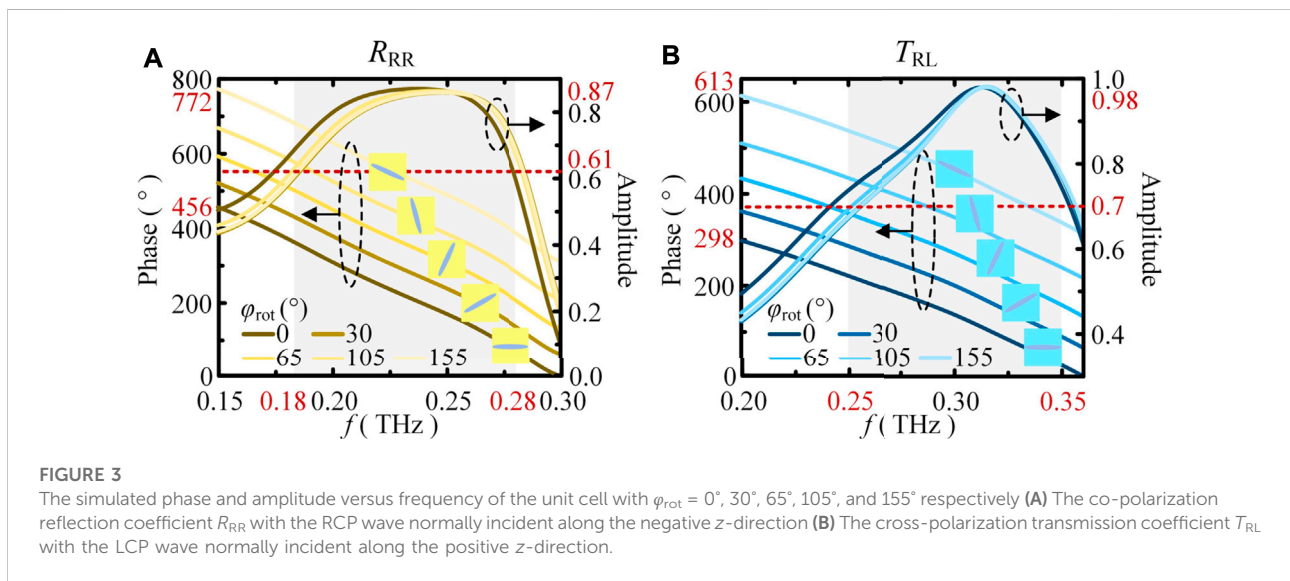
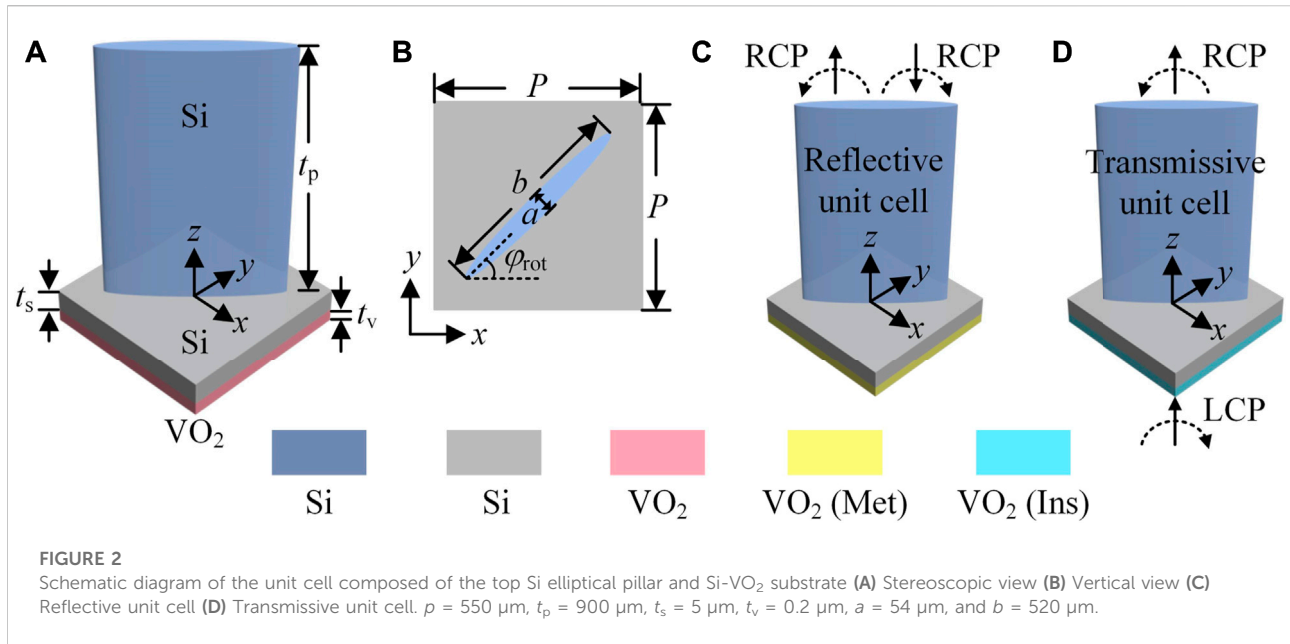


FIGURE 1

The schematic diagram for two-dimensional multichannel multiplexing combing with spatial and frequency domains is achieved by the reconfigurable dielectric metasurface which can work in both reflection and transmission modes (A) For reflective metasurface, 4×M-channel off-axis RCP plane waves with the frequency f_m and angle of incidence $\theta_i(f_m)$ ($m = 1, \dots, M$) are incident on the metasurface from the negative z-axis along negative x and y directions, and positive x and y directions respectively, RCP reflected waves are transformed into 4×M-channel orthogonal on-axis OAM beams with different topological charges ($l = l_1, l_2, l_3$, and l_4) or frequencies ($f = f_1$ to f_M) (B) Similarly, for the transmissive metasurface, 4×M-channel off-axis LCP plane waves are incident on the transmissive metasurface from the positive z-axis along with negative x and y directions, and positive x and y directions respectively, RCP transmitted waves are transformed into 4×M-channel orthogonal on-axis OAM beams with topological or frequency orthogonality.

respectively. Besides, the topological charges of these four groups of OAM beams are different from each other. Thus, it can be seen that 4×M-channel orthogonal on-axis beams with topological or frequency orthogonality are realized, and two-dimensional multichannel multiplexing combing with spatial and frequency domains by the reflective metasurface is achieved.

As shown in Figure 1B, the designed metasurface works in the transmission mode. Similarly, for the group 1 to group 4, 4×M-channel left-handed circularly polarized (LCP) plane waves with frequency f_m and angle of incidence $\theta_i(f_m)$ ($m = 1, \dots, M$) obliquely illuminate on the transmissive metasurface from the positive z-axis along negative x and y directions, as well as positive x and y directions respectively, in the direction



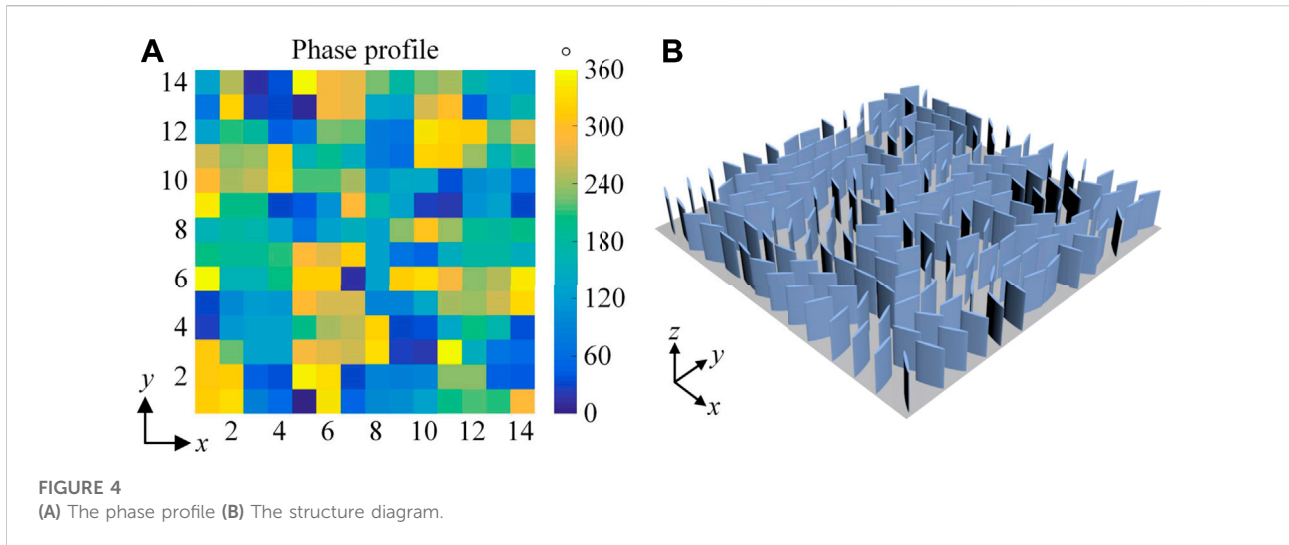
perpendicular to the metasurface, the cross-polarization transmitted waves (RCP transmitted wave) are transformed into $4 \times M$ -channel orthogonal on-axis OAM beams with topological or frequency orthogonality. Thus, two-dimensional multichannel multiplexing combing with spatial and frequency domains by the transmissive metasurface can be realized.

First, to generate the OAM beam with topological charge l , the phase profile φ_l of the metasurface should satisfy Eq. 1:

$$\varphi_l(x, y) = l \cdot \arctan \frac{y}{x}, l = 0, \pm 1, \pm 2, \dots \quad (1)$$

where (x, y) represents the arbitrary coordinate position on the metasurface and l represents the topological charge. It is worth noting that the topological charge of the plane wave is 0.

Then, according to the generalized laws of reflection and refraction [45], set the phase-gradient metasurface as the interface between the media one and 2. When the EM wave is incident on the metasurface from media one along the negative z -axis, the incidence angle α_i and reflected angle α_r should satisfy Eq. 2, and when the EM wave is incident on the metasurface from



media two along the positive z -axis, the incidence angle α_i and refracted angle α_t should satisfy Eq. 3:

$$\begin{aligned} \sin(\alpha_r) - \sin(\alpha_i) &= \frac{\lambda_0}{2\pi n_i} \frac{d\varphi_d(x)}{dx} \text{ or } \sin(\alpha_r) - \sin(\alpha_i) \\ &= \frac{\lambda_0}{2\pi n_i} \frac{d\varphi_d(y)}{dy} \end{aligned} \quad (2)$$

$$\begin{aligned} \sin(\alpha_t)n_t - \sin(\alpha_i)n_i &= \frac{\lambda_0}{2\pi} \frac{d\varphi_d(x)}{dx} \text{ or } \sin(\alpha_t)n_t - \sin(\alpha_i)n_i \\ &= \frac{\lambda_0}{2\pi} \frac{d\varphi_d(y)}{dy} \end{aligned} \quad (3)$$

where n_i and n_t are refractive indices of the media. $(d\varphi_d/dx)$ and $(d\varphi_d/dy)$ are constant gradients of phase discontinuity along the metasurface. If $n_i = 1$, $n_t = 1$, and $\alpha_i = 0^\circ$, the phase profile φ_d of the phase-gradient metasurface can be expressed as Eq. 4:

$$\varphi_d(x) = \pm \frac{2\pi}{D} \cdot x \text{ or } \varphi_d(y) = \pm \frac{2\pi}{D} \cdot y \quad (4)$$

where $D = M \cdot P$ is the super unit cell period along the phase gradient direction, P is the period of the unit cell, and M is the number of units constituting the super unit cell. α_r and α_t can be expressed as Eqs. 5,6:

$$\begin{aligned} \alpha_r(f) &= \arcsin\left(\frac{C}{2\pi f} \cdot \frac{d\varphi_d(x)}{dx}\right) \text{ or } \alpha_r(f) \\ &= \arcsin\left(\frac{C}{2\pi f} \cdot \frac{d\varphi_d(y)}{dy}\right) \end{aligned} \quad (5)$$

$$\begin{aligned} \alpha_t(f) &= \arcsin\left(\frac{C}{2\pi f} \cdot \frac{d\varphi_d(x)}{dx}\right) \text{ or } \alpha_t(f) \\ &= \arcsin\left(\frac{C}{2\pi f} \cdot \frac{d\varphi_d(y)}{dy}\right) \end{aligned} \quad (6)$$

where f is the incident wave frequency and C represents the EM wave velocity in the free space. α_r and α_t are related to f .

Therefore, according to Eqs. 1,4, when a plane wave with f is vertically incident on a reflective or transmissive metasurface, to generate four-channel off-axis beams deflected along $\pm x$ and $\pm y$ directions with α_r or α_t and different topological charges, the transfer function t of the metasurface should satisfy Eq. 7:

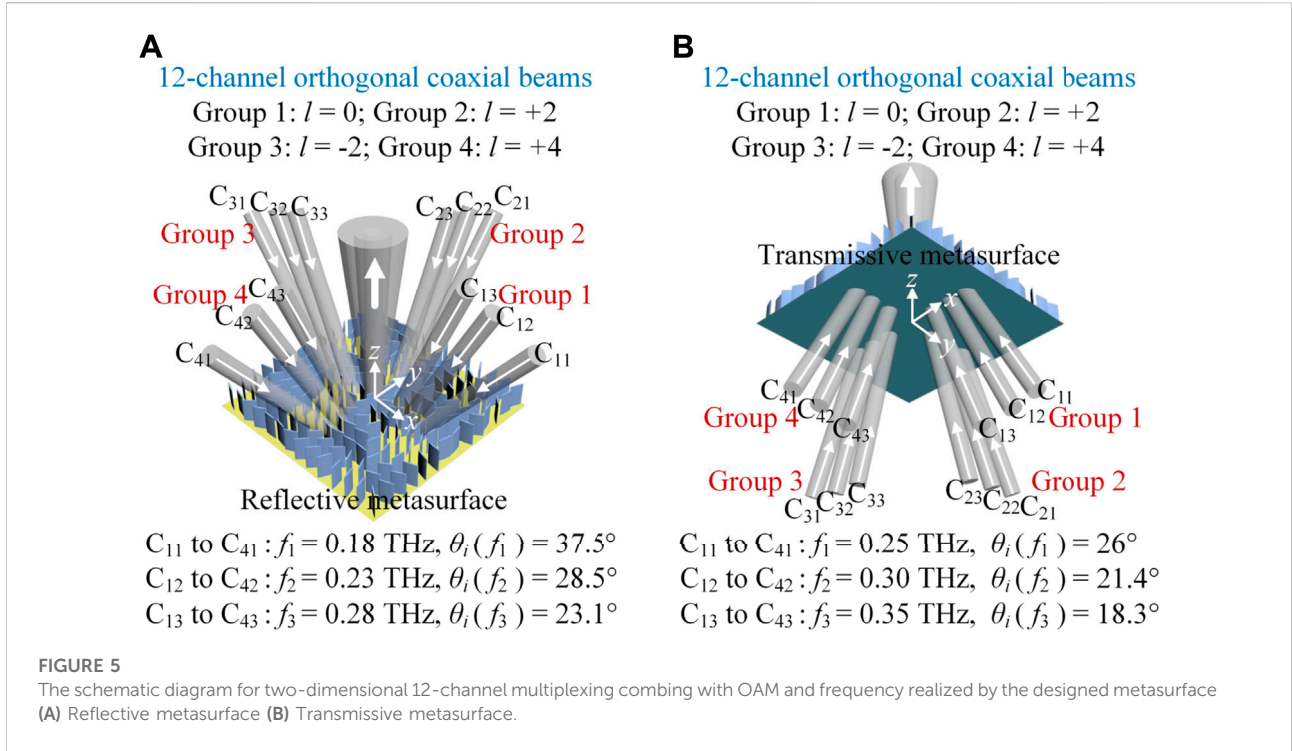
$$t = \sum_{m=1}^4 e^{j(\varphi_{lm} + \varphi_{dm})} \quad (7)$$

Next, according to Eq. 7, if four-channel off-axis plane beams are incident on the reflective metasurface from the negative z -direction or on the transmissive metasurface from the positive z -direction with f and the angle of incidence $\theta_i(f)$, the phase profile ϕ of the metasurface can be expressed as Eq. 8 [25, 44]. It is worth noting that for the reflective and transmissive metasurfaces, θ_i should satisfy Eqs. 5,6 respectively.

$$\phi(x, y) = \text{angle}(t) = \text{angle}\left(\sum_{m=1}^4 e^{j(\varphi_{lm} + \varphi_{dm})}\right) \quad (8)$$

Therefore, if the designed metasurface satisfies Eq. 8, the two-dimensional multichannel multiplexing can be achieved by this metasurface working in reflection or transmission mode.

Then, according to the PB phase principle (geometric phase principle) [43], when the unit cell rotates φ_{rot} clockwise, for the reflective unit cell, there is a phase shift (PB phase) which is as twice the rotation angle $2\varphi_{rot}$ between the RCP reflective wave and RCP wave incident from above the unit cell. For the transmissive unit cell, there is a PB phase $2\varphi_{rot}$ between the RCP transmitted wave and LCP wave incident from the back of the unit cell. Therefore, the $0-2\pi$ phase shift can be covered by rotating the unit cell from 0 to π and the proposed metasurface can be designed by the geometric phase principle. The rotation angle profile of the metasurface can be expressed as follows:



$$\varphi_{\text{rot}}(x, y) = \frac{\phi(x, y)}{2} \tag{9}$$

Moreover, in the THz region, according to the Drude model, the permittivity ϵ of VO₂ varying with angular frequency ω can be expressed as follows [37, 41]:

$$\epsilon(\omega) = \epsilon_{\infty} - \frac{\omega_p^2(\sigma)}{\omega^2 + i\gamma\omega} \tag{10}$$

$$\omega_p^2(\sigma) = \frac{\sigma}{\sigma_0} \omega_p^2(\sigma_0) \tag{11}$$

where $\epsilon_{\infty} = 12$ is the high frequency permittivity, $\omega_p^2(\sigma)$ is plasma frequency depending on the conductivity σ of VO₂, $\gamma = 5.75 \times 10^{13}$ rad/s is the collision frequency, $\omega_p(\sigma_0) = 1.4 \times 10^{15}$ rad/s with $\sigma_0 = 3 \times 10^3 \Omega^{-1}\text{cm}^{-1}$, and $\sigma = 2 \times 10^3$ s/cm or 2 s/cm with VO₂ in the metallic or insulator state respectively.

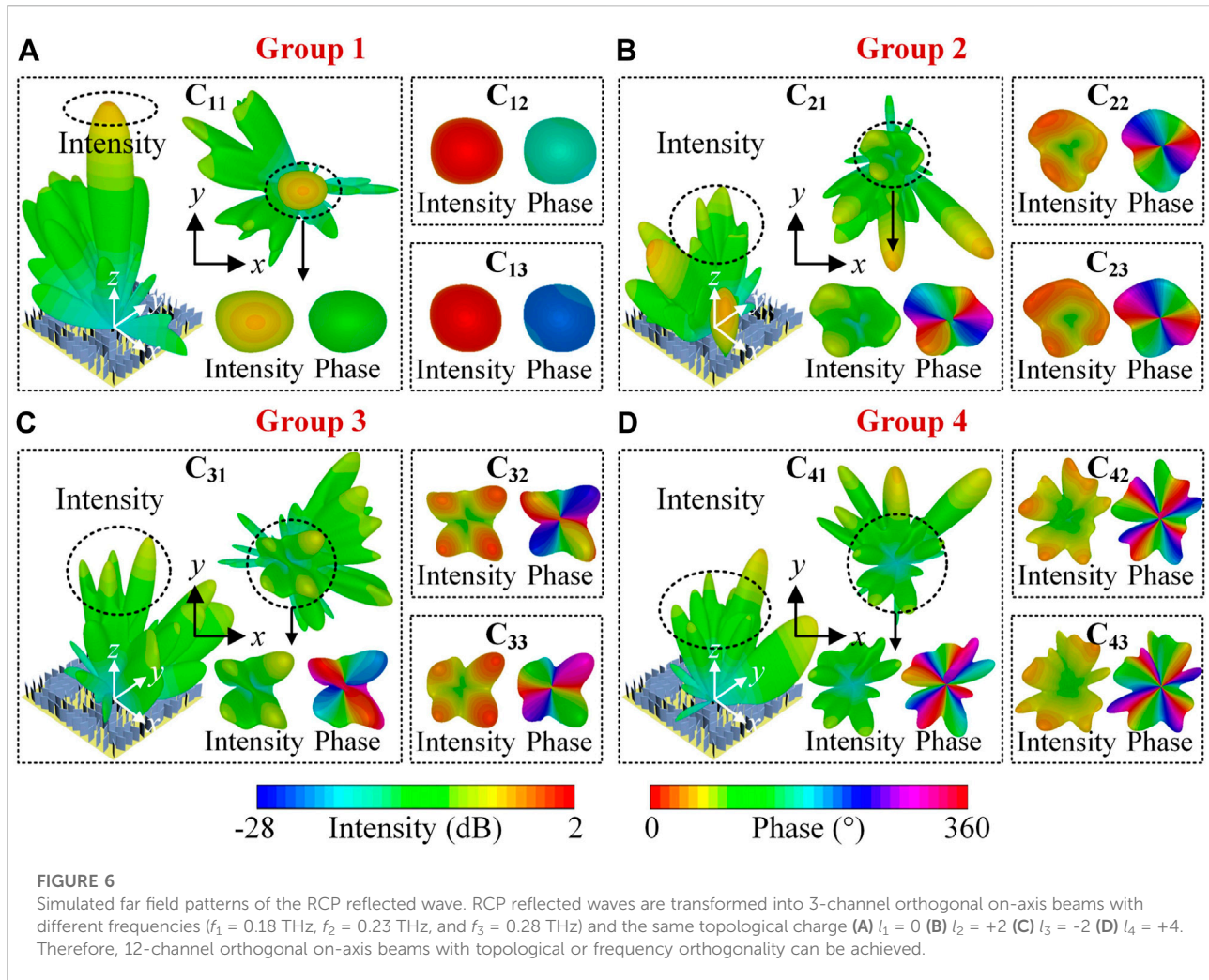
In summary, the required metasurface working in both reflection and transmission modes for two-dimensional multichannel multiplexing can be designed by Eq. 8, PB phase principle, and VO₂.

Unit cell

Figure 2 depicts the unit cell of the proposed reconfigurable dielectric metasurface. As shown in Figures 2A,B, the unit cell comprises top silicon ($\epsilon = 11.9$) elliptical pillar and Si-VO₂ substrate. It is worth noting that to distinguish the Si pillar

and the Si substrate, the different colors are used. The period of the unit cell is $p = 550 \mu\text{m}$, the height of the Si pillar is $t_p = 900 \mu\text{m}$, the thickness of the Si-VO₂ substrate is $t_s = 5 \mu\text{m}$ and $t_v = 0.2 \mu\text{m}$, and the minor and major axes of the ellipse are $a = 54 \mu\text{m}$ and $b = 520 \mu\text{m}$ respectively. The angle between the major axis and positive x -axis is φ_{rot} . As shown in Figures 2C,D, the unit cell can work in reflection and transmission modes by switching the VO₂ from the metallic state to the insulator state.

CST Microwave Studio is applied to investigate the unit cell numerically. Periodic boundaries and Floquet ports are employed along with the x - y and z directions. For the reflective and transmissive unit cell with VO₂ in metallic and insulator state, RCP and LCP waves are normally incident onto the unit cell along $-z$ and $+z$ directions, respectively. VO₂ is modeled by the Drude model by Eqs. 10,11. Besides, φ_{rot} changes from 0° to 180° . Figure 3 shows the simulated phase and amplitude of the co-polarization reflection coefficient R_{RR} and the cross-polarization transmission coefficient T_{RL} versus frequency with $\varphi_{\text{rot}} = 0^\circ, 30^\circ, 65^\circ, 105^\circ$, and 155° , respectively (Si substrate is hidden in the schematic diagram of the unit cell). The maximum amplitude of R_{RR} and T_{RL} are about 0.87 and 0.98. Therefore, the 3 dB bandwidth of the R_{RR} and T_{RL} are about 0.1 THz, and the operating frequency band is about 0.18–0.28 THz (The relative bandwidth is about 43.5%) and 0.25–0.35 THz (The relative bandwidth is about 36.7%) respectively. Besides, the phase shift is near-parallel and can cover $0-2\pi$ by rotating the unit cell from 0 to π in the operating frequency band. It is worth noting that based on the PB principle,



the required phase shift can also be satisfied under the oblique incident wave.

Metasurface

A reconfigurable dielectric metasurface consist of 14×14 unit cells with $M = 5$, $l_1 = 0$, $l_2 = +2$, $l_3 = -2$, and $l_4 = +4$ is designed for verification. The phase profile $\phi(x, y)$ and rotation angle profile $\varphi_{\text{rot}}(x, y)$ of the designed metasurface can be obtained by Equations 8, 9, respectively. The phase profile and structure diagram are shown in Figure 4.

When the metasurface works in the reflection mode with VO₂ in the metallic state, take $f_1 = 0.18$ THz, $f_2 = 0.23$ THz, and $f_3 = 0.28$ THz for example, the corresponding angle of incidences are $\theta_i(f_1) \approx 37.5^\circ$, $\theta_i(f_2) \approx 28.5^\circ$, and $\theta_i(f_3) \approx 23.1^\circ$ respectively, calculated based on Eq. 5. While the metasurface works in the transmissive mode with VO₂ in the insulator state, take $f_1 = 0.25$ THz, $f_2 = 0.3$ THz, and $f_3 = 0.35$ THz with $\theta_i(f_1) \approx 26^\circ$, $\theta_i(f_2)$

$\approx 21.4^\circ$, and $\theta_i(f_3) \approx 18.3^\circ$ respectively for examples, obtained based on Eq. 6. According to Figure 1, the schematic diagram for two-dimensional 12-channel multiplexing combining with OAM and frequency realized by the designed metasurface (Si substrate is hidden) is shown in Figure 5.

When the designed metasurface works in the reflection mode, simulated far-field patterns of the RCP reflected wave are shown in Figure 6. As shown in Figure 6A, for the channel C₁₁, the off-axis RCP plane wave is incident on the metasurface with f_1 and $\theta_i(f_1)$ along the negative x -axis, and an RCP reflected beam with a solid intensity profile and unchanged phase front is generated in the direction perpendicular to the metasurface. Therefore, the incident wave is transformed into a beam with f_1 and $l_1 = 0$. Similarly, for channel C₁₂ or C₁₃, the incident wave is transformed into a beam with f_2 or f_3 and $l_1 = 0$. Therefore, the generated 3-channel on-axis beams of group 1 are orthogonal with each other. As shown in Figure 6B, For group 2, when the incident RCP plane wave with f_m and $\theta_i(f_m)$ ($m = 1, 2$, and 3) obliquely illuminates on the metasurface along the negative

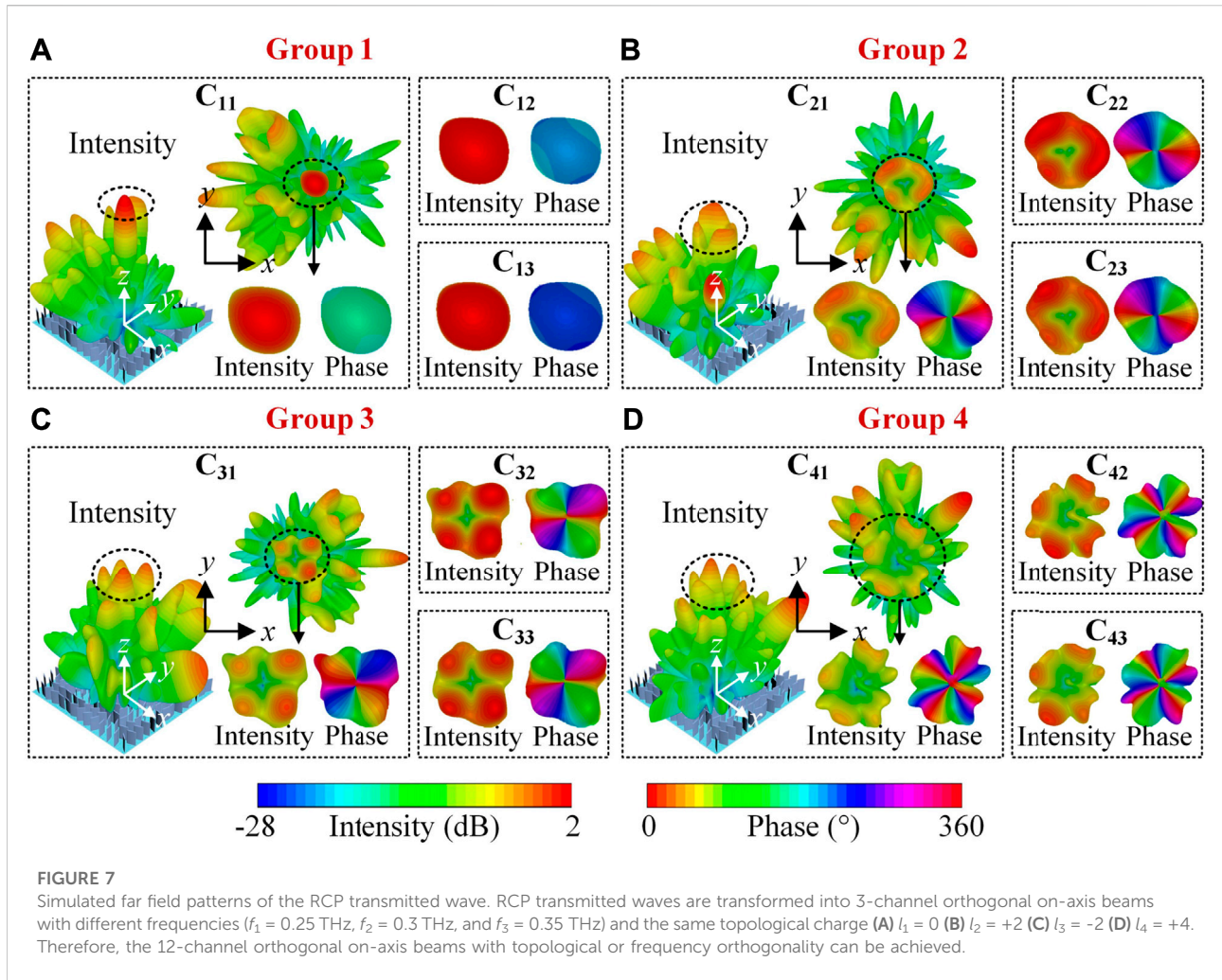


TABLE 1 The calculated variances σ^2 for different OAM modes.

OAM mode l	-5	-4	-3	-2	-1	0	+1	+2	+3	+4	+5
σ^2 of channel C_{23}	49.5	36.5	25.5	16.5	9.5	4.6	1.6	0.6	1.6	4.6	9.6
σ^2 of channel C_{43}	82.8	65.8	50.8	37.8	26.8	17.6	10.7	5.9	2.9	1.9	2.9

y -direction, an RCP reflected beam is generated in the direction perpendicular to the metasurface. Besides, the intensity profile is doughnut-shaped and the phase front changes 4π clockwise observing along the $+z$ direction. Therefore, incident waves are transformed into 3-channel orthogonal on-axis beams with different frequencies (f_1 , f_2 , and f_3) and $l_2 = +2$ respectively. In the same way, for group 3 or group 4, when off-axis incident RCP plane waves with f_m and $\theta_i(f_m)$ illuminate on the metasurface along $+x$ or $+y$ directions respectively, in the direction perpendicular to the metasurface,

RCP reflected waves are transformed into 3-channel orthogonal on-axis OAM beams with topological charge $l_3 = -2$ or $l_4 = +4$ (The intensity profile is doughnut-shaped and the phase front changes -4π or $+8\pi$ clockwise along the $+z$ direction). Besides, the topological charges of the four groups of beams are different from each other. Therefore, the 12-channel orthogonal on-axis beams with topological or frequency orthogonality can be achieved, and two-dimensional 12-channel multiplexing combing with spatial and frequency domains by the reflective metasurface can be realized. It is worth noting that there are strong sidelobes in the

far field patterns resulting from the angle-multiplexed metasurface design principle [42], which will affect the overall efficiency of the metasurface. In addition, according to the far field pattern, the maximum intensity of the generated beam is available. Take group 1 for example, the maximum value is about -4.26, 2.8, and 3.41 dB respectively.

When the designed metasurface works in the transmission mode, simulated far-field patterns of the RCP transmitted wave are shown in Figure 7. For group 1 to group 4, when 12-channel LCP plane waves with f_n and $\theta_i(f_n)$ obliquely illuminate on the metasurface from the positive z -axis along negative x and y directions, and positive x and y directions respectively, RCP transmitted wave are transformed into 12-channel orthogonal on-axis beams with topological orthogonality ($l_1 = 0, l_2 = +2, l_3 = -2$, and $l_4 = +4$) or frequency orthogonality ($f_1 = 0.25$ THz, $f_2 = 0.3$ THz, and $f_3 = 0.35$ THz). Therefore, two-dimensional 12-channel multiplexing combing with spatial and frequency domains by the transmissive metasurface can be realized. Similarly, take group 1 for example, the maximum intensity of the generated beam is about 2.56, 7.01, and 5.47 dB respectively.

In addition, the phase gradient method [46] can be used to measure the purity of the generated OAM mode based on the simulated far field phase. For the reflective metasurface, take channel C_{23} for example. The far field phase of the RCP reflected wave is sampled at a pitch angle of 5° and an interval of 1° in the spherical coordinate system. For the transmissive metasurface, take channel C_{43} for example. The far field phase of the RCP transmitted wave is sampled at a pitch angle of 10° and an interval of 0.5° . Table 1 shows the calculated variances σ^2 for different OAM modes. It can be seen that for channel C_{23} , when the topological charge l is set as $+2$ during calculation, the variance is the smallest and the purity is the highest. Therefore, the topological charge of the generated OAM beam is $+2$. Similarly, for channel C_{43} , when $l = +4$, the variance is the smallest and the purity is the highest. Therefore, the topological charge of the generated OAM beam is $+4$.

Based on the above results, two-dimensional 12-channel multiplexing combing with spatial and frequency domains by the reconfigurable dielectric metasurface is realized. Besides, the metasurface works in both reflection mode and transmission mode with the operating frequency band switching from 0.18–0.28 THz to 0.25–0.35 THz by tuning the VO_2 .

Conclusion

A terahertz reconfigurable dielectric metasurface embedded with VO_2 for two-dimensional multichannel multiplexing combing with spatial and frequency domains is presented in this paper. The metasurface works in both reflection mode and transmission mode by switching the VO_2 from the metallic state to the insulator state. For reflective metasurface, $4 \times M$ -channel off-axis

RCP plane wave with f_m and angle of incidence $\theta_i(f_m)$ ($m = 1, \dots, M$) illuminate on the metasurface from the negative z -axis along with negative x and y directions, and positive x and y directions respectively, in the direction perpendicular to the metasurface, RCP reflected waves are transformed into $4 \times M$ -channel orthogonal on-axis beams with topological orthogonality ($l = l_1, l_2, l_3$, and l_4) or frequency orthogonality ($f = f_1$ to f_M). For transmissive metasurface, $4 \times M$ -channel off-axis LCP plane waves are incident on the metasurface from the positive z -axis along with negative x and y directions, and positive x and y directions respectively, in the direction perpendicular to the metasurface, RCP transmitted waves are transformed into $4 \times M$ -channel orthogonal on-axis beams with topological or frequency orthogonality. A metasurface composed of 14×14 unit cells with $l_1 = 0, l_2 = +2, l_3 = -2$, and $l_4 = +4$ is designed for verification. The metasurface works in both reflection and transmission modes with the operating frequency band switching from 0.18–0.28 THz to 0.25–0.35 THz by tuning the state of VO_2 . When the metasurface works in the reflection or transmissive mode, take $f_1 = 0.18$ THz, $f_2 = 0.23$ THz, and $f_3 = 0.28$ THz, or $f_1 = 0.25$ THz, $f_2 = 0.3$ THz, and $f_3 = 0.35$ THz for examples. The simulation results show that two-dimensional 12-channel multiplexing combing with spatial and frequency domains by the metasurface is realized. The proposed metasurface has great potential in terahertz communications.

Data availability statement

The original contributions presented in the study are included in the article/supplementary material, further inquiries can be directed to the corresponding authors.

Author contributions

LW, YY, and LD conceived the work and suggested the outline of the article. LW, FG, ST, ZT, XZ, and JL carried out investigations and wrote the article.

Funding

This research was funded in part by the Natural Science Foundation of Hunan Province, grant number 2022JJ40114 and in part by the Research Foundation of Education Bureau of Hunan Province, grant number 21C0831.

Conflict of interest

The authors declare that the research was conducted in the absence of any commercial or financial relationships that could be construed as a potential conflict of interest.

Publisher's note

All claims expressed in this article are solely those of the authors and do not necessarily represent those of their affiliated

organizations, or those of the publisher, the editors and the reviewers. Any product that may be evaluated in this article, or claim that may be made by its manufacturer, is not guaranteed or endorsed by the publisher.

References

- Bukhari SS, Vardaxoglou J, Whittow W. A metasurfaces review: Definitions and applications. *Appl Sci (Basel)* (2019) 9:2727. doi:10.3390/app9132727
- Zhang LL, Li P, Song XW. Tunable wide-angle multi-band mid-infrared linear-to-linear polarization converter based on a graphene metasurface. *Chin Phys B* (2021) 30:127803. doi:10.1088/1674-1056/ac0cdd
- Wu JB, Shen Z, Ge SJ, Chen BW, Shen ZX, Wang TF, et al. Liquid crystal programmable insulator-to-metal transition in a grapheme metasurface. *Chin Phys B* (2021) 30:127803. doi:10.1088/1674-1056/ac0cdd
- Li Y, Lin J, Guo HJ, Sun WJ, Xiao SY, Zhou L. A tunable metasurface with switchable functionalities: From perfect transparency to perfect absorption. *Adv Opt Mater* (2020) 8:1901548. doi:10.1002/adom.201901548
- Tsilipakos O, Tasolamprou AC, Ptilakis A, Liu F, Wang XC, Mirmoosa MS, et al. Toward intelligent metasurfaces: The progress from globally tunable metasurfaces to software-defined metasurfaces with an embedded network of controllers. *Adv Opt Mater* (2020) 8:2000783. doi:10.1002/adom.202000783
- Follan TG, Fali A, White ST, Matson JR, Liu S, Aghamiri NA, et al. Reconfigurable infrared hyperbolic metasurfaces using phase change materials. *Nat Commun* (2018) 9:4371–7. doi:10.1038/s41467-018-06858-y
- Liu MK, Hwang HY, Tao H, Strikwerda AC, Fan K, Keiser GR, et al. Terahertz-field-induced insulator-to-metal transition in vanadium dioxide metamaterial. *Nature* (2012) 487:345–8. doi:10.1038/nature11231
- Li CL, Yu P, Huang YJ, Zhou Q, Wu J, Li Z, et al. Dielectric metasurfaces: From wavefront shaping to quantum platforms. *Prog Surf Sci* (2020) 95:100584. doi:10.1016/j.progsurf.2020.100584
- Winzer PJ. Spatial multiplexing in fiber optics: The 10x scaling of metro/core capacities. *Bell Labs Tech J* (2014) 19:22–30. doi:10.15325/BLTJ.2014.2347431
- Allen L, Beijersbergen MW, Spreeuw RJC, Woerdman JP. Orbital angular momentum of light and the transformation of Laguerre-Gaussian laser modes. *Phys Rev A (Coll Park)* (1992) 45:8185–9. doi:10.1103/PhysRevA.45.8185
- He JN, Wan ML, Zhang XP, Yuan SQ, Zhang LF, Wang JQ. Generating ultraviolet perfect vortex beams using a high-efficiency broadband dielectric metasurface. *Opt Express* (2022) 30:4806–16. doi:10.1364/OE.451218
- Fu B, Yu SX, Kou N, Ding Z, Zhang ZP. Design of cylindrical conformal transmitted metasurface for orbital angular momentum vortex wave generation. *Chin Phys B* (2022) 31:040703. doi:10.1088/1674-1056/ac3a65
- Zhang K, Wang YX, Burokur SN, Wu Q. Generating dual-polarized vortex beam by detour phase: From phase gradient metasurfaces to metagratings. *IEEE Trans Microw Theor Tech* (2021) 70:200–9. doi:10.1109/TMTT.2021.3075251
- Wang Y, Wang H, Su RF, Li SH, Tu XC, Wu JB, et al. Flexible bilayer terahertz metasurface for the manipulation of orbital angular momentum states. *Opt Express* (2021) 29:33445–55. doi:10.1364/OE.439370
- Wang YX, Zhang K, Yuan YY, Ding XM, Yang GH, Fu JH, et al. Generation of high-efficiency vortex beam carrying OAM mode based on miniaturized element frequency selective surfaces. *IEEE Trans Magn* (2019) 55:1–4. doi:10.1109/TMAG.2019.2919715
- Ou K, Li GH, Li TX, Yang H, Yu FL, Chen J, et al. High efficiency focusing vortex generation and detection with polarization-insensitive dielectric metasurfaces. *Nanoscale* (2018) 10:19154–61. doi:10.1039/C8NR07480A
- Jin ZW, Janoschka D, Deng JH, Ge L, Dreher P, Frank B, et al. Phylloxera-inspired nanosieves with multiplexed orbital angular momentum. *ELight* (2021) 1:5–11. doi:10.1186/s43593-021-00005-9
- Ha YL, Guo YH, Pu MB, Li X, Ma XL, Zhang ZJ, et al. Monolithic-Integrated multiplexed devices based on metasurface-driven guided waves. *Adv Theor Simul* (2021) 4:2000239. doi:10.1002/adts.202000239
- Liu MZ, Huo PC, Zhu WQ, Zhang C, Zhang S, Song MW, et al. Broadband generation of perfect Poincaré beams via dielectric spin-multiplexed metasurface. *Nat Commun* (2021) 12:2230–9. doi:10.1038/s41467-021-22462-z
- Mai QL, Wang CF, Wang XR, Cheng SH, Cheng ML, He YL, et al. Metasurface based optical orbital angular momentum multiplexing for 100 GHz radio over fiber communication. *J Lightwave Technol* (2021) 39:6159–66. doi:10.1109/JLT.2021.3097176
- Meng XS, Wu JJ, Wu ZS, Yang L, Huang L, Li X, et al. Erratum: "Generation of multiple beams carrying different orbital angular momentum modes based on anisotropic holographic metasurfaces in the radio-frequency domain" [Appl. Phys. Lett. 114, 093504 (2019)]. *Appl Phys Lett* (2019) 114:139902. doi:10.1063/1.5096976
- Feng Q, Kong XD, Shan MM, Lin YF, Li L, Cui TJ. Multi-orbital-angular-momentum-mode vortex wave multiplexing and demultiplexing with shared-aperture reflective metasurfaces. *Phys Rev Appl* (2022) 17:034017. doi:10.1103/PhysRevApplied.17.034017
- Yuan YY, Zhang K, Ratni B, Song QH, Ding XM, Wu Q, et al. Independent phase modulation for quadruplex polarization channels enabled by chirality-assisted geometric-phase metasurfaces. *Nat Commun* (2020) 11:4186–9. doi:10.1038/s41467-020-17773-6
- Zheng CL, Wang GC, Li J, Li JT, Wang SL, Zhao HL, et al. All-dielectric metasurface for manipulating the superpositions of orbital angular momentum via spin-decoupling. *Adv Opt Mater* (2021) 9:2002007. doi:10.1002/adom.202002007
- Li SQ, Li XY, Zhang L, Wang GX, Zhang LX, Liu ML, et al. Efficient optical angular momentum manipulation for compact multiplexing and demultiplexing using a dielectric metasurface. *Adv Opt Mater* (2020) 8:1901666. doi:10.1002/adom.201901666
- Chen SQ, Xie ZQ, Ye HP, Wang XR, Guo ZH, He YL, et al. Cylindrical vector beam multiplexer/demultiplexer using off-axis polarization control. *Light Sci Appl* (2021) 10:222–9. doi:10.1038/s41377-021-00667-7
- Wang L, Yang Y, Deng L, Hong WJ, Zhang C, Li SF. Terahertz angle-multiplexed metasurface for multi-dimensional multiplexing of spatial and frequency domains. *Adv Theor Simul* (2020) 3:2000115. doi:10.1002/adts.202000115
- Jiang ZH, Kang L, Hong W, Werner DH. Highly efficient broadband multiplexed millimeter-wave vortices from metasurface-enabled transmit-arrays of subwavelength thickness. *Phys Rev Appl* (2018) 9:064009. doi:10.1103/PhysRevApplied.9.064009
- Hu YZ, Tong MY, Xu ZJ, Cheng XG, Jiang T. Spatiotemporal terahertz metasurfaces for ultrafast all-optical switching with electric-triggered bistability. *Laser Photon Rev* (2021) 15:2000456. doi:10.1002/lpor.202000456
- Kim Y, Wu PC, Sokhoyan R, Mauser K, Glauddell R, Shirmanesh GK, et al. Phase modulation with electrically tunable vanadium dioxide phase-change metasurfaces. *Nano Lett* (2019) 19:3961–8. doi:10.1021/acs.nanolett.9b01246
- Urade Y, Fukawa K, Miyamaru F, Okimura K, Nakanishi T, Nakata Y. Dynamic inversion of planar-chiral response of terahertz metasurface based on critical transition of checkerboard structures. *Nanophotonics* (2022) 11:2057–64. doi:10.1515/nanoph-2021-0671
- Tripathi A, Kruk S, John J, Zhang Z, Nguyen HS, Berguiga L, et al. Tunable Mie-resonant dielectric metasurfaces based on VO₂ phase-transition materials. *ACS Photon* (2021) 8:1206–13. doi:10.1021/acsp Photonics.1c00124
- Yan DX, Feng QY, Yuan ZW, Meng M, Li XJ, Qiu GH, et al. Wideband switchable dual-functional terahertz polarization converter based on vanadium dioxide-assisted metasurface. *Chin Phys B* (2022) 31:014211. doi:10.1088/1674-1056/ac05a7
- Shu FZ, Wang JN, Peng RW, Xiong B, Fan RH, Gao YJ, et al. Electrically driven tunable broadband polarization states via active metasurfaces based on joule-heat-induced phase transition of vanadium dioxide. *Laser Photon Rev* (2021) 15:2100155. doi:10.1002/lpor.202100155
- Kou W, Shi WQ, Zhang YX, Yang ZQ, Chen T, Gu JQ, et al. Terahertz switchable focusing planar lens with a nanoscale vanadium dioxide integrated metasurface. *IEEE Trans Terahertz Sci Technol* (2021) 12:13–22. doi:10.1109/TTHZ.2021.3105576
- Wu GZ, Jiao XF, Wang YD, Zhao ZP, Wang YB, Liu JG. Ultra-wideband tunable metamaterial perfect absorber based on vanadium dioxide. *Opt Express* (2021) 29:2703–11. doi:10.1364/OE.416227

37. Liu WW, Song ZY. Terahertz absorption modulator with largely tunable bandwidth and intensity. *Carbon* (2021) 174:617–24. doi:10.1016/j.carbon.2020.12.001
38. Kang L, Wu YH, Werner DH. Active terahertz spin Hall effect in vanadium dioxide metasurfaces. *Opt Express* (2021) 29:8816–23. doi:10.1364/OE.421283
39. Li J, Li JT, Zhang YT, Li JN, Yang Y, Zhao HL, et al. All-optical switchable terahertz spin-photonic devices based on vanadium dioxide integrated metasurfaces. *Opt Commun* (2020) 460:124986. doi:10.1016/j.optcom.2019.124986
40. Chen L, Zhao L, Hao Y, Liu WY, Wu Y, Wei ZC, et al. Metasurface spiral focusing generators with tunable orbital angular momentum based on slab silicon nitride waveguide and vanadium dioxide (VO₂). *Nanomaterials* (2020) 10:1864. doi:10.3390/nano10091864
41. Liu XB, Wang Q, Zhang XQ, Li H, Xu Q, Xu YH, et al. Thermally dependent dynamic meta-holography using a vanadium dioxide integrated metasurface. *Adv Opt Mater* (2019) 7:1900175. doi:10.1002/adom.201900175
42. Wang L, Yang Y, Deng L, Hong WJ, Zhang C, Li SF. Vanadium dioxide embedded frequency reconfigurable metasurface for multi-dimensional multiplexing of terahertz communication. *J Phys D Appl Phys* (2021) 54:255003. doi:10.1088/1361-6463/abf166
43. Ding XM, Monticone F, Zhang K, Zhang L, Gao DL, Burokur SN, et al. Ultrathin Pancharatnam–Berry metasurface with maximal cross-polarization efficiency. *Adv Mater* (2015) 27:1195–200. doi:10.1002/adma.201405047
44. Tan H, Deng J, Zhao RZ, Wu X, Li GX, Huang LL, et al. A free-space orbital angular momentum multiplexing communication system based on a metasurface. *Laser Photon Rev* (2019) 13:1800278. doi:10.1002/lpor.201800278
45. Yu NF, Genevet P, Kats MA, Aieta F, Tetienne JP, Capasso F, et al. Light propagation with phase discontinuities: Generalized laws of reflection and refraction. *Science* (2011) 334:333–7. doi:10.1126/science.1210713
46. Qi X, Zhang ZY, Zong XZ, Que XF, Nie ZP, Hu J. Generating dual-mode dual-polarization OAM based on transmissive metasurface. *Sci Rep* (2019) 9:97–12. doi:10.1038/s41598-018-36677-6